Influence of the annual cycle of sea surface temperature on the monsoon onset

Xingwen Jiang[1,2,3] and Jianping Li[2]

Received 23 October 2010; revised 2 February 2011; accepted 8 March 2011; published 21 May 2011.

[1] Differing from the traditional focus on land-sea thermal contrasts, this paper examines the influence of the annual cycle of sea surface temperature (SST) on the monsoon onset. It is found that SST is a major driver of tropical circulations in the atmospheric boundary layer. In the trade wind regions, the annual cycle of SST involves a shift in the warmest SST axis (WSSTA) between two local maxima on either sides of the equator or slight movement of WSSTA north of the equator; consequently, WSSTA has little effect on the regional meridional SST gradient and wind direction. However, in the monsoon regions, the annual cycle of SST is characterized by an abrupt northward jump of WSSTA, resulting in a marked change in regional meridional SST gradient and consequent onset of winds. The onset of the southwesterlies lags behind the abrupt northward jump of WSSTA. As an example, the climatological onset of the monsoon in the Bay of Bengal (BOB) shows that the abrupt northward jump of WSSTA is caused by an increase in SST in the BOB, leading to the monsoon onset after about 2 pentads. SST shows a maximum before the monsoon onset, contributing to destabilization of the atmosphere. A strong meridional SST gradient occurs between BOB and south of the equator after the abrupt northward jump of WSSTA, associated with cross-equatorial flow in the eastern Indian Ocean. Case studies indicate that an abrupt northward jump in WSSTA from the equator to north of 10°N is a good omen for the monsoon onset.

Citation: Jiang, X., and J. Li (2011), Influence of the annual cycle of sea surface temperature on the monsoon onset, *J. Geophys. Res.*, *116*, D10105, doi:10.1029/2010JD015236.

1. Introduction

[2] Monsoon systems show considerable temporal variability on a wide range of scales. The most important subseasonal phenomenon is the monsoon onset [*Webster et al.*, 1998], which is characterized by an abrupt change in winds, precipitation, convection, large-scale circulation, and other phenomena [*Lau and Yang*, 1997; *Webster et al.*, 1998; *Wang and Lin Ho*, 2002; *Li and Zhang*, 2009]. In recent decades, many studies have analyzed various aspects of the monsoon onset, including its definition, spatiotemporal evolution, possible causes, and interannual variability [*He et al.*, 1987; *Yanai et al.*, 1992; *Lau and Yang*, 1997; *Webster et al.*, 1998; *Wang and Lin Ho*, 2002; *Zhang et al.*, 2002; *Li and Zhang*, 2009; *Wang et al.*, 2009].

[3] The continental-scale land-sea thermal contrast has long been regarded as the main reason for monsoonal circulation [*Webster et al.*, 1998]; thus many studies have investigated the cause of monsoon onset from the perspective of the reversal in temperature gradient between land and sea. Using first GARP Global Experiment (FGGE) data, *He et al.* [1987] and *Yanai et al.* [1992] showed that the onset of the Asian monsoon in 1979 involved two distinct stages, the Southeast Asian monsoon onset and the Indian monsoon onset. The two onsets were caused mainly by a reversal in the meridional temperature gradient due to warming of the upper troposphere over the Asian landmass. *Wu and Zhang* [1998] reported that the Asian summer onset first occurs over the Bay of Bengal (BOB) in early May, directly linked to thermal forcing by the Tibetan Plateau. A study of the Australian monsoon revealed that the thermal contrast due to differential heating between land and sea acts as a seasonal preconditioning for the monsoon onset [*Hung and Yanai*, 2004]. Furthermore, the area-averaged upper tropospheric meridional temperature gradient has been proposed as an index with which to define the summer onset over the BOB [*Mao and Wu*, 2007]. Interannual variability in the monsoon onset is related to the thermal condition over the Tibetan Plateau during the premonsoon season because the reversal in the thermal contrast between land and sea is controlled mainly by heating over land [*Mao and Wu*, 2007].

[4] Sea surface temperature (SST) also has a strong influence on monsoonal variability [*Webster et al.*, 1998; *Wang*,

[1]College of Atmospheric Sciences, Lanzhou University, Lanzhou, China.
[2]National Key Laboratory of Atmospheric Sciences and Geophysical Fluid Dynamics, Institute of Atmospheric Physics, Chinese Academy of Sciences, Beijing, China.
[3]Institute of Plateau Meteorology, China Meteorological Administration, Chengdu, China.

0148-0227/11/2010JD015236

2006]. In the case of the monsoon onset, the climatologic characteristics of the Asian monsoon show that warm regional SST contributes to the monsoon onset [*Wu and Wang*, 2001; *Ueda*, 2005]. For example, the seasonal northeastward march of the warmest SST tongue favors the northeastward movement of the monsoon trough and the region of high convective instability [*Wu and Wang*, 2001]. The interannual variability of the monsoon onset is affected by remote SST, with late (early) monsoon onset over most parts of Asia during El Niño (La Niña) events [*Joseph et al.*, 1994; *Lau and Yang*, 1997; *Wu and Wang*, 2000; *Zhang et al.*, 2002; *Mao and Wu*, 2007]. Few previous studies have examined the relationship between the monsoon onset and the annual cycle of SST, despite the fact that the monsoon is closely related to SST and that both show strong subseasonal variability.

[5] The monsoon exists in an aqua planet that considers the seasonal evolution of SST [*Yano and McBride*, 1998; *Chao and Chen*, 2001]. Aqua planet experiments with a seasonally varying SST anomaly indicate that the monsoon onset should be preceded by SST forcing away from the equator [*Yano and McBride*, 1998]. *Chao* [2000] and *Chao and Chen* [2001] interpreted the monsoon as an intertropical convergence zone (ITCZ) located far from the equator and proposed that the existence of the ITCZ is not dependent on the land-sea thermal contrast. In reality, the extent of the tropical monsoons is surrounded by the positions of the ITCZ in summer and winter [*Li and Zeng*, 2005], which is the result of the two driving forcings of the tropical monsoon, the seasonal variation of the planetary thermal convection due to the seasonal variation of solar radiation caused by the obliquity of the Earth, and the seasonal variation of the semipermanent planetary waves due to the thermal contrast between ocean and continent [*Zeng and Li*, 2002]. The tropical monsoon onset might be mainly interpreted as an abrupt change in the location of the ITCZ from an equatorial trough flow regime to the monsoon trough flow. The ITCZ favors a location with high SST, indicating that the SST peak located away from equator is a precondition for the monsoon onset. Previous simulations using a general circulation model showed that the annual cycles of SST and solar heating have an influence on monsoonal circulation [*Sud et al.*, 2002; *Lestari and Iwasaki*, 2006]. The seasonal march of SST destabilizes the stratification and induces a jump in the ITCZ from the Southern Hemisphere to Northern Hemisphere, thereby contributing to the monsoon onset [*Lestari and Iwasaki*, 2006].

[6] The results of the above numerical model studies suggest that the annual cycle of SST has an influence on the monsoon onset and that the meridional SST peak should be located away from the equator before the onset. However, the real monsoon onset is a complicated, coupled ocean-atmosphere-land phenomenon, giving rise to the following questions. What are main characteristics of the annual cycle of SST? What role does it play in the real monsoon onset? Can the variations of meridional SST peak be used as a predictor for the monsoon onset? In addition, the observation studies suggest that the local warm SST contribute to the monsoon onset. What are the relative contributions of the warm SST and the SST peak located away from the equator to the monsoon onset?

[7] In the present study, we focus on the relationship between the annual cycle of SST and the monsoon onset. The remainder of the paper is organized as follows. In section 2, we present the data sets analyzed in this study, along with the analysis methods. In section 3, we describe the climatological annual cycle of SST and wind in the lower troposphere for various regions, in order to examine the influence of the annual cycle of SST on wind. In section 4, focusing on the BOB as an example, we investigate the influence of the annual cycle of SST on the monsoon onset. In section 5, we analyze the characteristics of the processes of monsoon onset in the BOB for early and late onset years, in order to verify whether the key climatological features are seen these years, and investigate relative contribution of magnitude of warm SST and meridional SST gradient to the monsoon onset. Finally, a summary and discussion of the results are provided in section 6.

2. Data and Methodology

[8] The daily 925 hPa wind data used in the present analysis were derived from the National Center for Environmental Prediction/National Center for Atmospheric Research (NCEP/NCAR) reanalysis [*Kalnay et al.*, 1996]. We used Climate Prediction Center (CPC) pentad (5-day mean) Merged Analysis Precipitation data (CMAP) [*Xie and Arkin*, 1997], derived by merging rain gauge observations, five different satellite estimates, and the outputs of numerical models. The daily Outgoing Longwave Radiation (OLR) of the National Oceanic and Atmospheric Administration (NOAA) was provided by the Climate Diagnostics Center (CDC) [*Liebmann and Smith*, 1996]. Daily SST data are from the NOAA Optimum Interpolation (OI) analysis [*Reynolds et al.*, 2007]. The spatial resolution is 2.5° (latitude and longitude) for wind, OLR, and CMAP and 0.25° for SST. All the data cover the period from 1986 to 2008. The observed data sets were all constructed for the 23-year (1986–2008) mean for climatological analysis. The SST data were averaged to grids at a resolution of 1° (latitude and longitude) to remove small-scale disturbances. All the daily time series were smoothed using a 5-day running average.

[9] The absolute angle between vectors of the prevailing surface wind is calculated as follows [*Li and Zeng*, 2000; *Zhang and Li*, 2008]:

$$\beta_j = \beta(V_j, V_R) = \arccos\left(\frac{(V_j, V_R)}{|V_j||V_R|}\right), (j = 1, \ldots, 365)$$

where V_j is the daily wind vector and V_R is the reference wind vector at the same point. We selected the January climatological wind vector as the reference wind vector. The norm (V_j, V_R) represent the vector product, and $|\cdot|$ denotes the module of the wind vector; thus β_j essentially measures the difference in the angle of wind vectors between a specific day and corresponding winter, and $0 \le \beta_j \le 180°$. The absolute angle describes the nature of variations in wind direction and performs well in representing the abrupt transition of the wind onset and withdrawal of the monsoon [*Zhang and Li*, 2008, 2010; *Li and Zhang*, 2009].

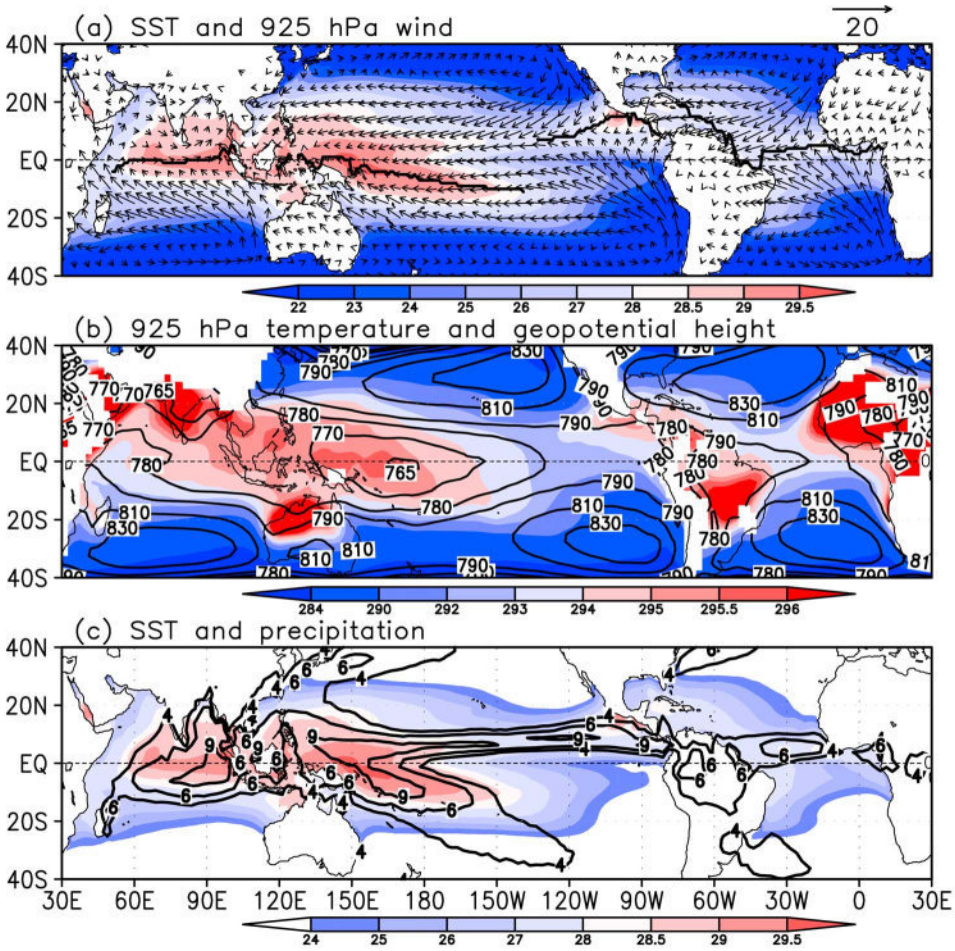

Figure 1. Climatological annual mean of (a) SST (°C; shading) and wind vectors at 925 hPa; (b) air temperature (K; shading) and geopotential height (gpm; contours) at 925 hPa; and (c) SST (°C; shading) and precipitation (mm d^{-1}; contours). The thick, solid black line in Figure 1a represents the position of the meridional SST maximum.

[10] To conveniently describe the warmest SST, we define the warmest SST axis (WSSTA) as the global meridional SST maximum in tropical oceans between 20°S and 20°N.

3. Relationship Between Wind and SST in the Tropics

3.1. Annual Mean

[11] If the annual cycle of SST is simply a response to the annul cycle of solar radiation, the annual mean SST should have a maximum at the equator; however, as shown in Figure 1a, the WSSTA is located north of the equator in the eastern Pacific and Atlantic and south of the equator in the central Pacific. Forced by the asymmetric SST, the ITCZ is located north of the equator in the eastern Pacific and Atlantic and south of the equator in the central Pacific, associated with northward and southward cross-equatorial flows (CEFs), respectively. These patterns have been observed in previous studies and interpreted as a result of ocean-atmosphere coupling induced by the geometries of the continents [*Mitchell and Wallace*, 1992; *Xie*, 1994; *Xie and Philander*, 1994; *Philander et al.*, 1996].

[12] There are two processes by which the convection tends to occur over areas with warm SST. First, the warmer SST acts to enhance the moist static stability, thereby contributing to convection. As shown in Figure 1c, the pattern of the center of maximum precipitation largely corresponds to the pattern of the warmest SST, except for in the southeast Pacific (120°W–150°W, 5°W–15°N). Second, SST affects the air temperature via turbulent flow mixing in the atmospheric boundary layer, thereby affecting pressure. Figure 1b shows the annual mean temperature and geopotential height at 925 hPa, revealing a near-perfect correspondence between SST and 925 hPa temperature. Consequently, high (low) pressure is associated with cold (warm) SST in the boundary layer, meaning that air moves to the warmer SST, resulting in convection and enhanced precipitation.

[13] *Lindzen and Nigam* [1987] used a theoretical model to analyze the correlation between a disturbed SST gradient and convergence. Their results showed that flows forced directly by SST. Of note, regions of warm SST in the climatology are consistent with regions of convergence over tropical oceans (Figure 2a). The convergence is mostly ascribed to the longitudinal gradient in meridional wind within the tropics,

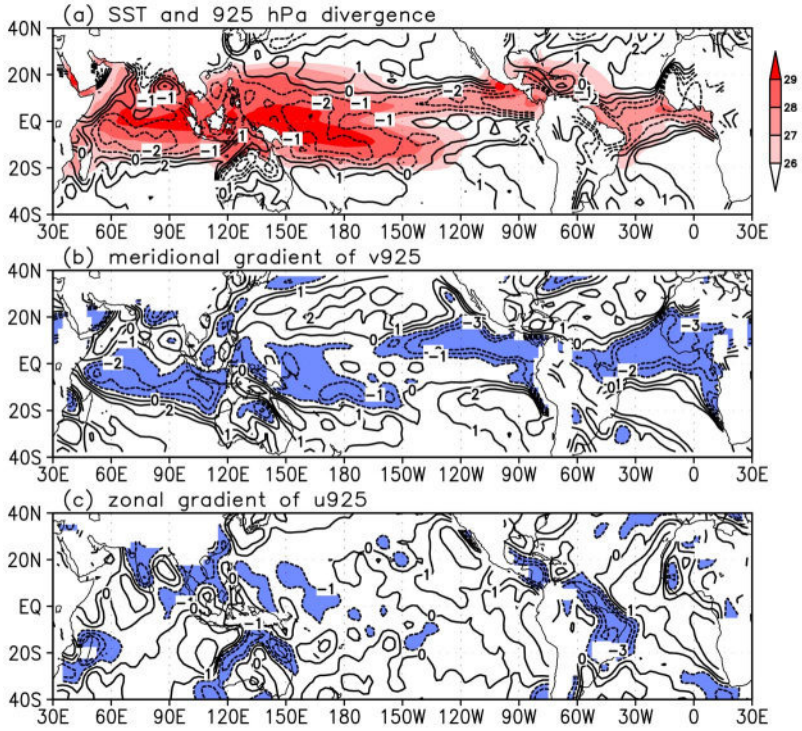

Figure 2. Climatological annual mean of (a) SST (°C; shading) and divergence (10e-5 s^{-1}; contours) of wind vectors at 925 hPa; (b) the meridional gradient (10e-5 s^{-1}; contours) of the longitudinal component of wind at 925 hPa (v925); and (c) the zonal gradient (10e-5 s^{-1}; contours) of the latitudinal component of wind at 925 hPa (u925). The blue areas represent areas that divergence value less than 1.0.

except in the western Pacific, where the latitudinal gradient in zonal wind cannot be ignored (Figures 2b and 2c). Figure 1a shows that this convergence pattern arises from that the meridional SST gradient (MSSTG) is greater than the latitudinal SST gradient, except in the western Pacific. Therefore MSSTG has a strong influence on the meridional wind and convergence in the tropics, with northerly and southerly winds on the north and south sides of the warm SST, respectively.

3.2. January and July

[14] Figure 3a and 3b shows the climatological SST and 925 hPa wind in January and July, respectively. WSSTA are located north of the equator in the eastern Pacific and Atlantic during January and July, associated with northward CEFs. In the western Pacific, WSSTA shifts from the Southern Hemisphere in January to the Northern Hemisphere in July, associated with southward and northward CEFs, respectively. In the central Pacific, SST at the equator is colder than in adjacent areas, which have warm SSTs of similar magnitude in both hemispheres; thus there is no clear CEF. The pattern in the central Pacific in January is the same as that in July. Strong CEFs occur in the Indian Ocean (IO) during both January and July, although WSSTA are located close to the equator.

[15] In the tropics, the transitions in meridional wind correspond to the transitions in SST, except for the IO. This exception in the IO is due in part to monsoonal circulation caused by the strongest land–sea thermal contrast observed worldwide, which arises because the largest continent on Earth is located north of the IO; this is why researchers emphasize the effects of the land–sea thermal contrast in explaining the development of monsoonal circulation [*He et al.*, 1987; *Yanai et al.*, 1992; *Webster et al.*, 1998; *Wu and Zhang*, 1998]. However, at the onset stage, SST has a greater effect on monsoonal circulation than does the thermal contrast, as discussed below. Changes in the magnitude and location of warm SST between January and July are accompanied by corresponding changes in low-pressure centers, bands of maximum precipitation, and convergent centers (figure not shown). With the shift in WSSTA from the southwest Pacific in January to the northwest Pacific in July, the longitudinal gradient is changed in the tropics. Here, we focus on the influence of MSSTG on wind and convergence because the effect of MSSTG is more important than that of the latitudinal SST gradient described above.

3.3. Annual Cycle

[16] In this section we divide the tropical ocean into several subsectors based on the above analyses and regional differences in the monsoon. We identify three subsectors in the monsoon region: the Arabian Sea (AS, 55°E–75°E), the BOB (85°E–95°E), and the western Pacific (WS, 120°E–150°E). We also recognize three subsectors in the trade wind region: the central Pacific (CP, 120°W–180°W), the eastern Pacific (EP, 90°W–120°W), and the Atlantic (10°W–50°W).

[17] Figure 4 shows the climatological annual cycle of longitudinally averaged SST and 925 hPa wind in the monsoon region. WSSTA shows an abrupt northward jump (ANJ) and abrupt southward retreat (ASR), as well as

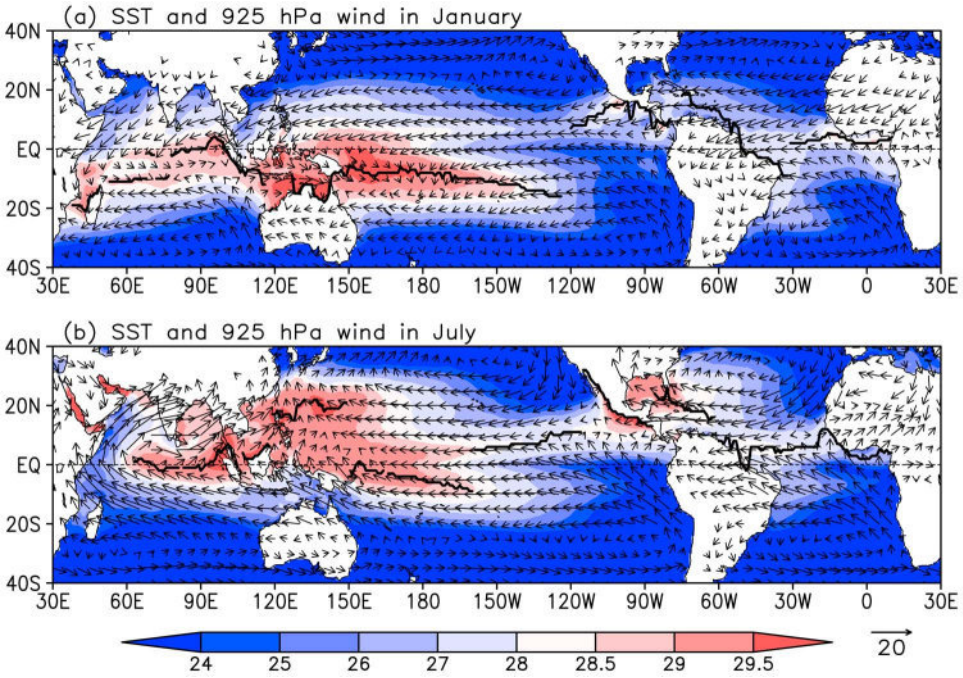

Figure 3. Climatological mean of SST (°C; shading) and wind vectors at 925 hPa for (a) January and (b) July, solid black line represents the position of the meridional SST maximum.

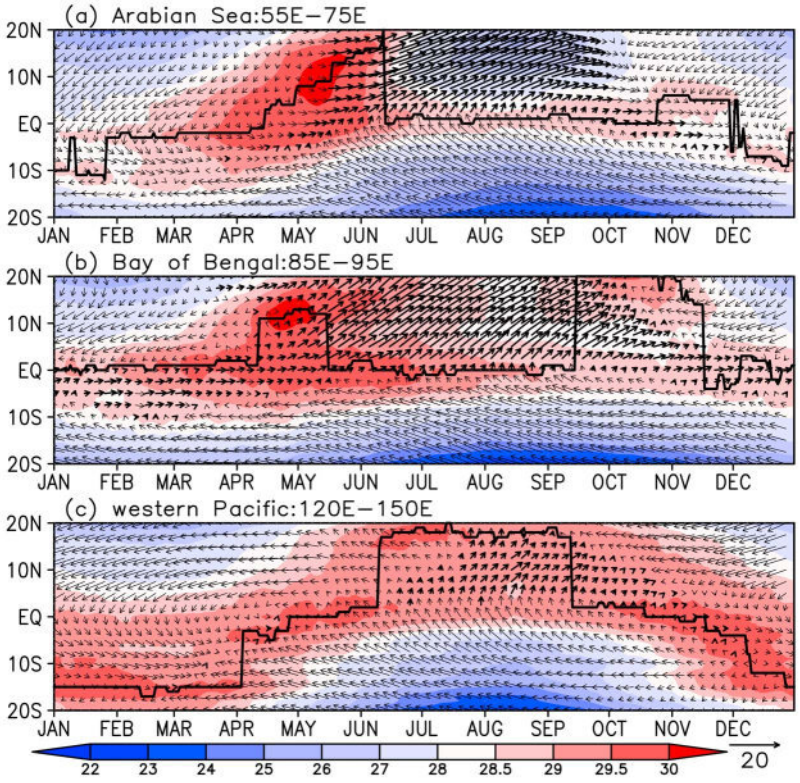

Figure 4. Latitude–time diagrams of climatological longitudinally averaged SST (°C; shading) and wind vectors at 925 hPa in the monsoon region. Thick arrows represent southwesterlies, and the thick, solid black line represents the position of the meridional SST maximum.

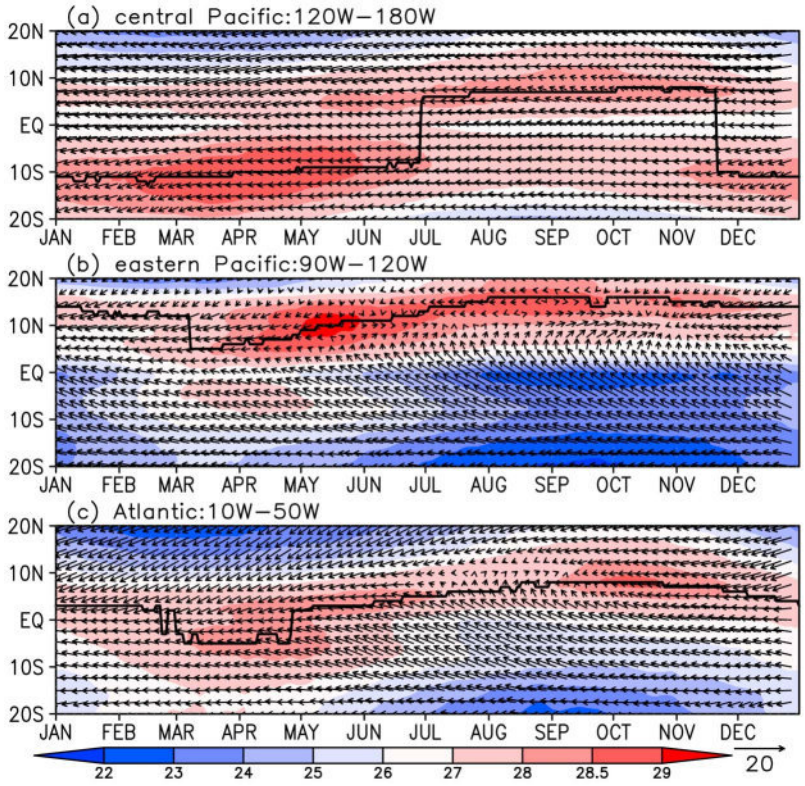

Figure 5. Latitude–time diagrams of climatological longitudinally averaged SST (°C; shading) and wind vectors at 925 hPa in the trade wind region. The thick, solid black line represents the position of the meridional SST maximum.

stagnancy. In the AS sector, WSSTA is close to the equator before mid-April and then jumps northward, step by step. In mid-May, WSSTA is at 13°N and then stagnates for about 25 days around this latitude until the ASR occurs in early June, involving a return to the equator. WSSTA stagnates at the equator from mid-May to late October and then jumps northward to 6°N, stagnating at this latitude until another ASR. WSSTA stagnates at around 10°S during December to January.

[18] In the BOB sector, WSSTA is stagnant around the equator year-round, except for two stages. First, WSSTA is stagnant at around 12°N during early April to mid-May, associated with an ANJ and ASR. Second, WSSTA is stagnant in the northern BOB, associated with an ANJ in mid-September and an ASR in mid-November. In the WP sector, there occur two ANJs and one ASR. WSSTA jumps northward, from 16°S to 3°S, in early April and then to the equator in early May, jumping to 18°N in early June. WSSTA retreats southward in early September, from 18°N to the equator, and then moves slowly to 16°S.

[19] In the Northern Hemisphere portions of the three sectors, the annual cycle of winds involves alternating southwesterlies and northeasterlies, with the onset of southwesterly winds being later than the ANJ of WSSTA (Figure 4). The northward CEF occurs after the ANJ of WSSTA, from the equator to north of 10°N. Southwesterlies occur prior to the ANJ of WSSTA in the northern AS and BOB during April to May. These winds originate from subtropical regions or are induced by the local land–sea thermal contrast, being distinct from the southern southwesterlies, and cannot be regarded as the southwesterly wind of the monsoon. The impact of the ANJ of WSSTA in mid-September in the BOB is discussed later. The ANJ of WSSTA from the equator to north of 10°N first occurred in the BOB, followed by the AS and finally the WP. Therefore the earlier the regional WSSTA jumps from the equator to north of 10°N, the earlier the onset of southwesterlies; however, the magnitude of the lag time of the onset of southwesterlies behind the ANJ of WSSTA differs among the regions.

[20] Figure 5 shows the climatological annual cycle of longitudinally averaged SST and 925 hPa wind in the trade wind region. Compared with the monsoon regions, the seasonal variability in SST and ANJ of WSSTA are less pronounced. In the CP sector, WSSTA stagnates at around 6°N during late June to late November and at around 11°S at other times of the year. WSSTA in the EP sector is located north of the equator year-round, moving northward during early March to late July and thereafter remaining stagnant at around 15°N. In the Atlantic sector, WSSTA is located south of the equator only during late February to later April; it moves slowly northward, to north of the equator, during late April to late August and moves southward during late October to December.

[21] In the trade wind region, the annual cycle of WSSTA is not associated with a significant change in MSSTG or wind because of the unique horizontal patterns of SST and the small movement in WSSTA. There exist two local SST maxima separated by a cold SST minimum on the equator in

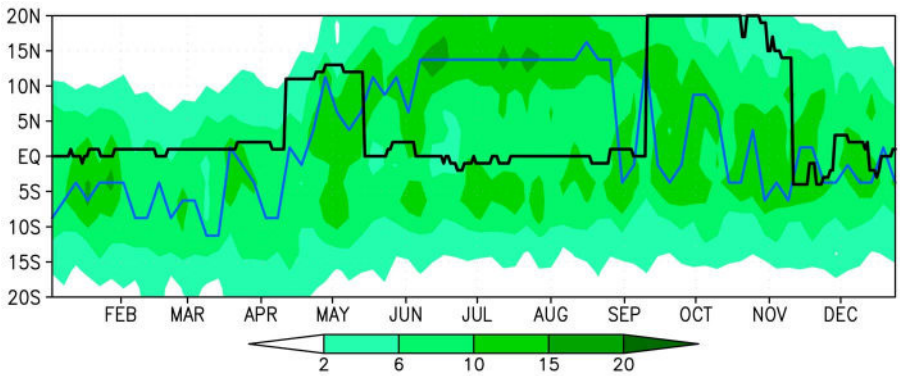

Figure 6. Latitude–time diagram of climatological longitudinally averaged precipitation (mm d^{-1}) between 85°E and 95°E. The black (blue) line represents the position of the meridional SST (precipitation) maximum.

the trade wind region. As shown in Figure 5a, the ANJ of WSSTA in the CP represents the shift between the two local SST maxima; it does not change MSSTG on either side of the equator and induces only a slight change in the thermal contrast between the Southern and Northern Hemispheres, resulting in a minor change to wind strength and direction. In the EP and Atlantic sectors, as reflected by the movement of WSSTA over a small latitudinal range, the annual cycle of SST change affects the magnitude of MSSTG, rather than its direction, meaning that few regions experience a change in wind direction. In the EP, the strongest CEF occurred in September, caused by the maximum temperature difference between the two local SST maxima. The weakest CEF occurred in March and April, associated with the minimum difference in temperature. Clear changes in wind direction are seen on both sides of WSSTA as it moves slowly northward during early March to early August. In the Atlantic, the strength of CEF is dependent on the difference in SST between areas south and north of the equator. Therefore the movement of WSSTA gives rise to a change in wind direction and strength that is dependent on the change in MSSTG.

[22] In the monsoon regions the occurrence of the ANJ of WSSTA, before the monsoon onset, results in marked changes in not only the local MSSTG but also in the interhemisphere temperature contrast (Figure 4), thereby inducing CEF and the onset of southwesterlies. Figure 4b shows that an ANJ of WSSTA occurs in mid-September in the BOB. It is difficult to identify the direct influence of the jump; however, compared with the transition of wind in the AS and WP, the retreat of the southwesterly wind occurs later in the BOB. Thus the ANJ of WSSTA may contribute to maintenance of the southwesterly wind during the process of monsoon withdrawal in the BOB.

[23] At approximately 20 days after the onset of southwesterly wind, WSSTA retreated southward to the equator, although strong southwesterlies are seen in the BOB and AS. These winds highlight the influence of the land-sea thermal contrast in driving the monsoonal circulation, although it is important not to overlook the importance of SST in this regard. The annual cycle of SST has a strong influence on local wind in the trade wind region, where the influence of the land-sea thermal contrast is relatively weak. The jump by WSSTA to north of 10°N occurs earlier than the reversal of the longitudinal temperature gradient in the AS and BOB sectors, as reported in previous studies [*Li and Yanai*, 1996; *Mao and Wu*, 2007]. Therefore SST plays an important role in the process of monsoon onset.

4. Climatological Characteristics of Monsoon Onset in the BOB

[24] In this section, focusing on the BOB, we investigate the spatiotemporal characteristics of SST, wind, and precipitation during the monsoon onset process and examine how the monsoon onset is related to the annual cycle of SST.

[25] Figure 6 shows the climatological annual cycle of longitudinally averaged precipitation in the BOB sector. At approximately 2 pentads after the ANJ of WSSTA in mid-April, the precipitation band located south of the equator shows an abrupt jump to the BOB, corresponding to the onset of southwesterly wind. After WSSTA has retreated to the equator in mid-May, the precipitation band shifts northward and persists until it returns to the equator in mid-September. Of note, a precipitation band is located south of the equator year-round, probably related to the warm SST band at the equator.

[26] Because the monsoon onset is a complicated process, it is appropriate to use several variables in representing the onset. Following *Li and Zhang* [2009], we selected wind and its zonal and meridional components, precipitation, and OLR to represent the monsoon onset. As shown in Figure 7a, the amplitude of the absolute angle of wind vectors shows an initially slow increase, remaining below 30° up to early April, before showing a sudden increase to a stable state above 150° in mid-April. In early April, we see a reversal in zonal wind from easterly to westerly and a reversal in meridional wind from northerly to southerly. However, the wind speeds are low until a sudden increase in late April (Figure 7b). Precipitation that exceeds the January average (2.9 mm d^{-1}) more than 5 mm d^{-1} first occurs in the 24th pentad (Figure 7c). OLR first falls below 235 Wm^{-2} in late April, remaining below this value during summer (Figure 7d).

[27] According to *Wang and Lin Ho* [2002] and *Li and Zhang* [2009], the onset of wind occurs in mid-April, with

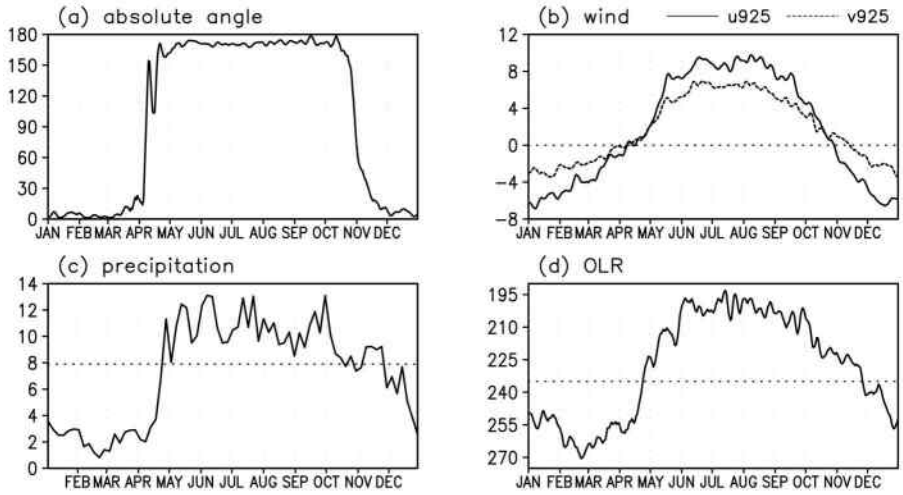

Figure 7. Latitude–time diagrams of the climatological area (5°N–15°N, 85°E–95°E) averaged (a) absolute angle (degree) of wind vectors at 925 hPa, (b) zonal (ms^{-1}; solid line; u925) and meridional (ms^{-1}; dashed line; v925) components of wind at 925 hPa, (c) precipitation (mm d^{-1}), and (d) OLR (Wm^{-2}).

the onset of zonal and meridional winds in early April, the onset of precipitation during the 24th pentad, and the onset of OLR in late April. The timing of onset differs among these variables, although the onset of precipitation is coincident with the onset of OLR, with both occurring later than the onset of wind-related variables. This difference in timing reflects the fact that the southwesterly of the monsoon in the BOB is contaminated by local circulation induced by the local land–sea thermal contrast; however, the sudden increase in wind speed is consistent with the onset of OLR and precipitation. The above analyses indicate that the monsoon onset in the BOB occurred during the 24th pentad.

[28] Figure 8 shows the climatological pentad-average SST and 925 hPa wind during the process of monsoon onset in the BOB. Prior to the ANJ of WSSTA, anticyclonic circulation occurs over the BOB and AS, and southwesterlies occur in the equatorial central IO. WSSTA is located either over the equator or south of it (Figure 8a). WSSTA shows a sudden jump to the central BOB during the 21st pentad but remains south of the equator in the AS sector (figure not shown). In the 22nd pentad, SST shows a sudden increase, with a result that the WSSTA is located entirely in the BOB, and southwesterlies emerge to the southwest of the BOB (Figure 8b). During the 23rd pentad, SST continues to

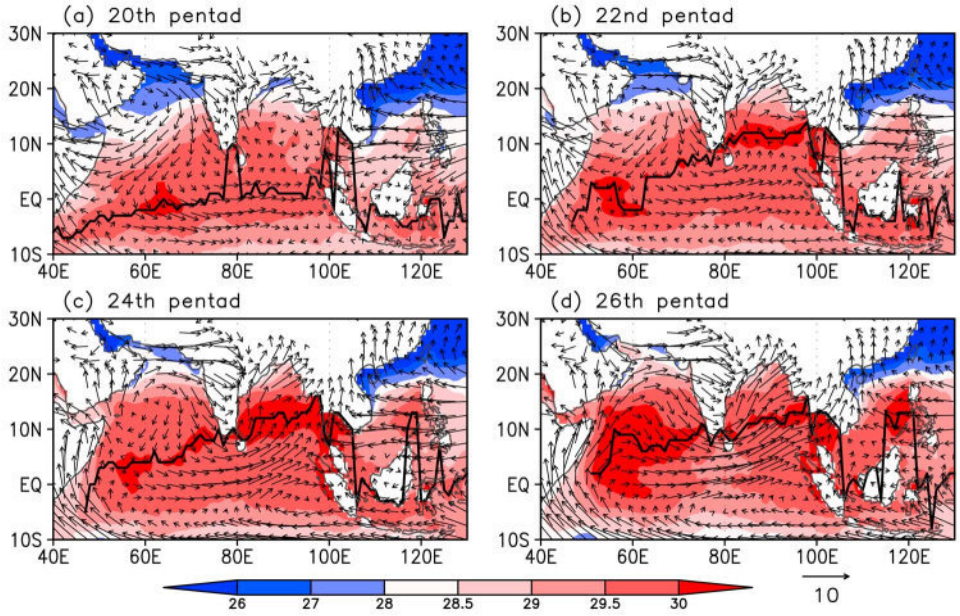

Figure 8. Climatological pentad-mean SST (°C; shading) and wind vectors at 925 hPa. The thick, solid black line represents the position of the meridional SST maximum.

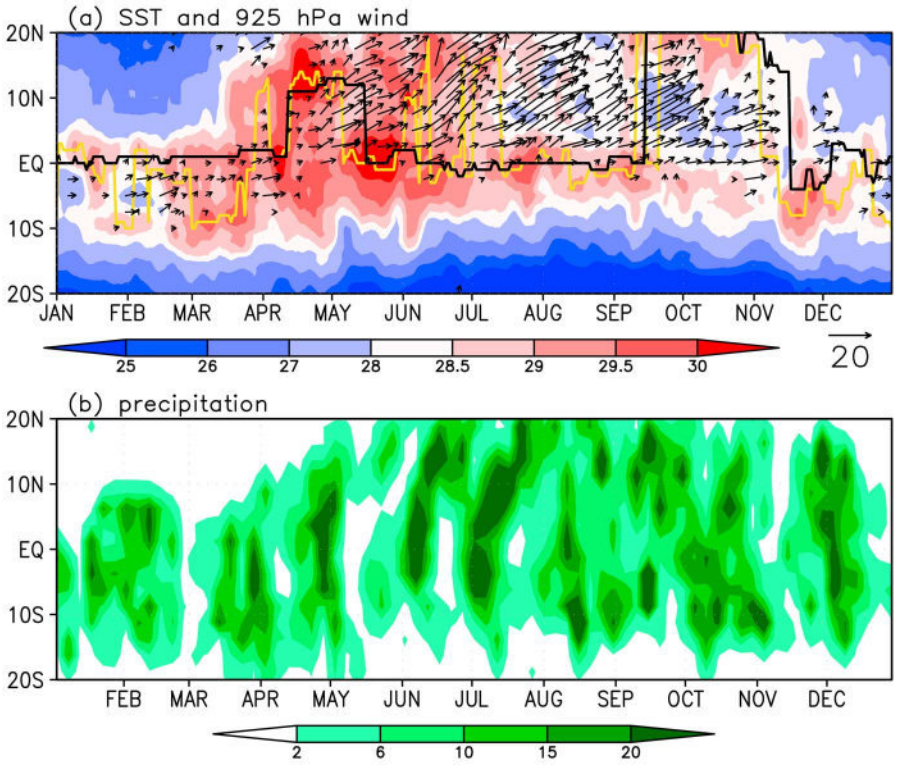

Figure 9. Latitude–time diagrams of longitudinally averaged (a) SST (°C; shading) and wind at 925 hPa and (b) precipitation (mm d^{-1}) between 85°E and 95°E in 1996. The black (yellow) line represents the position of the meridional SST maximum for the climatology (for 1996).

increase and the southwesterlies strengthen. During the 24th pentad, SST reaches a maximum, warm SST (>30°C) covers the central and southern BOB, southwesterlies prevail over the southern BOB, and strong CEF occurs in the equatorial eastern IO, resulting in the monsoon onset (Figure 8c). At this time, anticyclonic circulation persists in the AS, and WSSTA is located near the equator. After the monsoon onset (Figure 8d), SST shows a rapid decrease and southwesterlies move northward over the BOB. In the AS, the warm SST (>30°C) covers the entire southern part of the region, and WSSTA is located far from the equator. CEF weakens in the equatorial eastern IO and strengthens in the western IO.

[29] SST affects convection by destabilizing the atmosphere and convergence [*Wu and Wang*, 2001; *Fu et al.*, 2006; *Wu*, 2010]. Prior to the monsoon onset, SST reaches a maximum and exceeds 30°C in the BOB, contributing to destabilization of the atmosphere. In addition, a strong MSSTG exists between the BOB and south of the equator, leading to CEF and convergence. The MSSTG affects the CEF, as indicated by the fact that soon after the monsoon onset, SST shows a decrease in the BOB and MSSTG weakens between the BOB and south of the equator, resulting in a weaker CEF.

[30] The anticyclonic circulations over the BOB, prior to the monsoon onset, result in reduced wind speed and dry weather, thereby contributing to the SST increase and acting in favor of the monsoon onset. After the monsoon onset, in contrast, wind speed is enhanced and the cloud fraction increases, leading to a decrease in SST as a consequence of enhanced evaporation and reduced shortwave radiation flux at the sea surface, thereby inhibiting convection and CEF. Therefore the monsoon onset is a coupled ocean–atmosphere process, and SST has an important influence on the monsoon onset but not on the long-term maintenance of monsoonal circulation.

5. Case Studies

[31] The above investigation was based on the climatology. It is also important to consider interannual variability of the relationship between SST and the monsoon onset. In this context, we investigate the monsoon onset in the BOB for early and late onset years.

5.1. Monsoon Onset in the BOB During 1996

[32] Figure 9 shows the annual cycle of wind, SST, and precipitation in the BOB sector for 1996. WSSTA shifts between the equator and 10°S prior to a northward jump to north of 10°N in mid-April, where it persists until early May, followed by a retreat to the equator. Then, the WSSTA is generally located in the equator until another persistent northward displacement of WSSTA occurs during mid-September to late October. The annual cycle of WSSTA is overall the same as its climatology, although with some differences, such as the persistent time of WSSTA north of 10°N. Moreover, there are some disturbs of WSSTA, which shifts from the equator to the BOB. The onset of south-

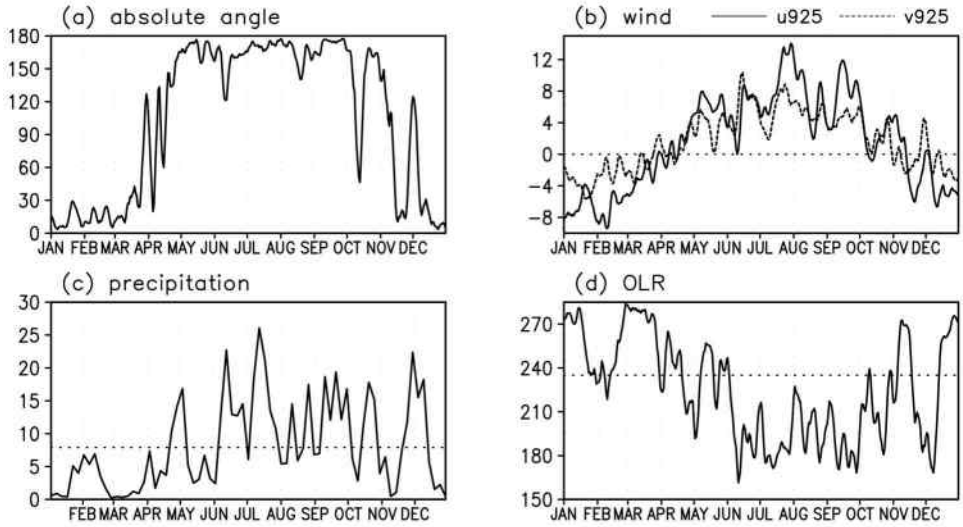

Figure 10. Latitude–time diagrams of the area (5°N–15°N, 85°E–95°E) averaged (a) absolute angle (degrees) of wind vectors at 925 hPa, (b) zonal (ms^{-1}; solid line; u925) and meridional (ms^{-1}; dashed line; v925) components of wind at 925 hPa, (c) precipitation (mm d^{-1}), and (d) OLR (Wm^{-2}) in 1996.

westerlies occurs in mid-April, earlier than the climatology. Precipitation shows a clear low-frequency oscillation and northward propagation. In mid-April, the precipitation maximum shifts from the equator to the BOB, corresponding to the commencement of the rainy season in the BOB.

[33] Figure 10 shows the annual cycle of the area-averaged absolute angle, zonal and meridional wind, precipitation, and OLR in the BOB in 1996. The absolute angle is generally less than 30° during January to March and then oscillates strongly about 90° prior to a sudden increase to a new, persistent state above 120° in mid-April. The reversal in persistent zonal wind from easterly to westerly and a reversal in meridional wind from northerly to southerly occur in mid-April. Precipitation that exceeds the January average more than 5 mm d^{-1} occurs in the 23rd pentad and is maintained for the subsequent 2 pentads, flowed by less precipitation about 4 mm d^{-1} during early May to early June. Of note, the less precipitation only takes place in the southern BOB (Figure 9b). During the period from mid-April to late November, OLR is generally less than 235 Wm^{-2}, excepting a short period from early May to early June. All of these features indicate that the time of monsoon onset is mid-April, earlier than the climatology.

[34] Figure 11 shows the pentad-mean SST and 925 hPa wind in the monsoon onset process in 1996. Prior to the WSSTA jump to the BOB, it is located south of the equator, associated with slow wind in the BOB and the equatorial eastern IO (Figure 11a). In the 21st pentad, SST increase in the BOB and the WSSTA jump northward, associated with southwesterlies around Sri Lanka (Figure 11b). There is convergence of southwesterlies and northeasterlies in the central BOB. In the 22nd pentad, warm SST (>30°C) covers most of the BOB (Figure 11c). Southwesterlies prevail in the southern BOB, accompanied by CEF in the equatorial eastern IO. Then, southwesterlies are further strengthened and dominate the BOB by 24th pentad, associated with strong CEF near Somali (Figure 11d).

5.2. Monsoon Onset in the BOB During 1998

[35] Figure 12 shows the annual cycle of wind, SST, and precipitation in the BOB sector for 1998. WSSTA is located at the equator prior to a northward jump to north of 10°N in late April, where it persists until late May, followed by a retreat to the equator. Then, the WSSTA is generally located in the equator until another persistent northward displacement of WSSTA occurs during mid-September to mid-October. The time of ANJ of WSSTA is later than its climatology. The onset of southwesterlies occurs in mid-May, also later than its climatology. In mid-May, the precipitation maximum shifts from the equator to the BOB, corresponding to the commencement of the rainy season in the BOB.

[36] Figure 13 shows the annual cycle of area-averaged absolute angle, zonal and meridional wind, precipitation, and OLR in the BOB in 1998. The magnitude of the absolute angle is generally less than 30° during January to Mid-April, and subsequently oscillations about 90° prior to a suddenly increase in mid-May to a new, persistent state above 150° (Figure 13a). The reversal in persistent zonal wind from easterly to westerly and a reversal in meridional wind from northerly to southerly occur in mid-May (Figure 13b). Precipitation exceeds the January average more than 5 mm d^{-1} during the 27 pentad and remains generally above this level until mid-November (Figure 13c). OLR is generally less than 235 Wm^{-2} from early May to mid-November (Figure 13d). The monsoon component onsets are generally during mid-May, later than the climatology.

[37] Figure 14 shows the pentad-mean SST and 925 hPa wind in the monsoon onset process for 1998. Prior to the jump of WSSTA to the BOB, the warm SST is located at the equator and anticyclonic circulation dominates the BOB, accompanied by westerlies in the equatorial central IO (Figure 14a). During the 24th pentad, WSSTA jumps to the central BOB due to an increase in SST, associated with westerlies extending to the equatorial eastern IO and

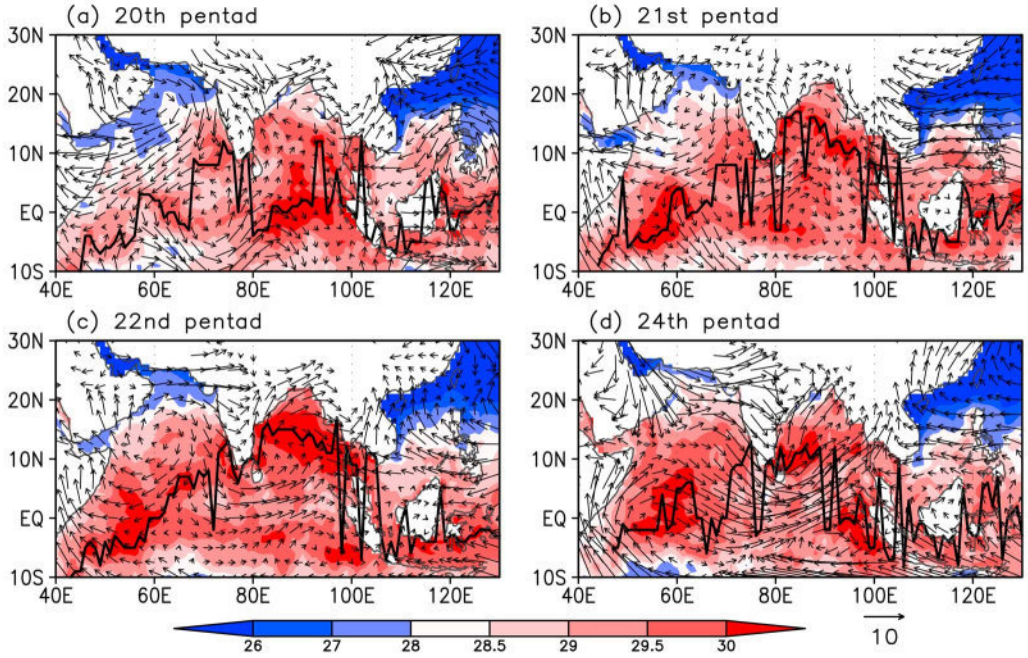

Figure 11. Pentad-mean SST (°C; shading) and wind vectors at 925 hPa in 1996. The thick, solid black line represents the position of the meridional SST maximum.

southwesterlies around Sri Lanka (Figure 14b). During the 25th pentad, warm SST (>31.5°C) covers the central BOB, leading to WSSTA entirely located in the BOB, accompanied by strengthen westerlies in the equatorial central IO (figure not shown). During the 26th pentad, WSSTA further jumps northward in the eastern BOB, and CEFs emerge in the equatorial eastern IO, accompanied by convergence in the southern BOB (Figure 14c). During the 27th pentad, WSSTA is located at the northern BOB, a cyclone forms in the southeastern BOB, and southwesterlies prevail in the southern BOB, associated with strong CEFs in the equatorial eastern and western IO (Figure 14d). During the 28th pentad, the cyclone moves northward to the northeastern India, strong southwesterlies dominate the entire BOB, and magnitude of WSSTA decreases in the northern BOB (figure not shown).

[38] The two cases show some common and different characteristics. The common characteristics are that SST increases in the BOB before the monsoon onset, leading to the ANJ of WSSTA. Then, westerlies strengthen in the equatorial central IO and CEF emergence in the equatorial eastern IO, contributing to the convergence in the southern BOB. After the onset of southwesterlies, SST decreases in the BOB, resulted in ASR of WSSTA to the equator. Formation of the Somali CEF is later than the monsoon onset in the BOB. These features are the same as the climatology.

[39] The different features are that the two cases are early and late onsets, respectively. The time of ABJ of WSSTA prior to the monsoon onset in 1996 is earlier than that in 1998, corresponding to the monsoon onset. However, the lag time of the monsoon onset behind the ANJ of WSSTA in 1996 is shorter than that in 1998. Although there are warm SSTs in the BOB before the monsoon onset, magnitudes of the SSTs are different. The SST in 1998 is higher than that in 1996.

[40] As mentioned in the above sections, the ANJ of WSSTA can trigger convection by two ways. One is that warm SST destabilizes the atmosphere. The other is that the MSSTG drives the convergence in the atmospheric boundary layer. The different characteristics of early and late onsets show that the ANJ of WSSTA trigger convection mostly by MSSTG rather than magnitude of warm SST. There are CEF in the equatorial eastern IO and southerlies in southern BOB after the ANJ of WSSTA, contributing to convergence. If the monsoon onset depends on the magnitude of warm SST, monsoon onset in 1998 would be earlier because the magnitude of SST before the onset is greater than that in 1996 or its climatology. Moreover, the climatology of monsoon onset in BOB indicates that SST before monsoon onset is just above 30°C. As shown in Figure 6, prior to the monsoon onset in the BOB, precipitation maximum is along the equator, where SST is lower than 30°C. Correlation analysis between SST and convection in IO suggests that the most favorable value of SST for organized deep convection is about 29.0°C [*Gadgil*, 2003]. Thus the monsoon onset depends mostly on the MSSTG rather than the magnitude of warm SST.

[41] Moreover, as shown in Figures 8d, 11d, and 14d, latent heat released from convective condensation further strengthens monsoon circulation following the Gill model [*Gill*, 1980].

6. Conclusion and Discussion

6.1. Conclusion

[42] The climatological characteristics of tropical SST and wind from 1986 to 2008 indicate that tropical circulation in the atmospheric boundary layer was driven primarily by SST. The zone of warm SST corresponds to a zone of convergence and precipitation maximum. The convergence

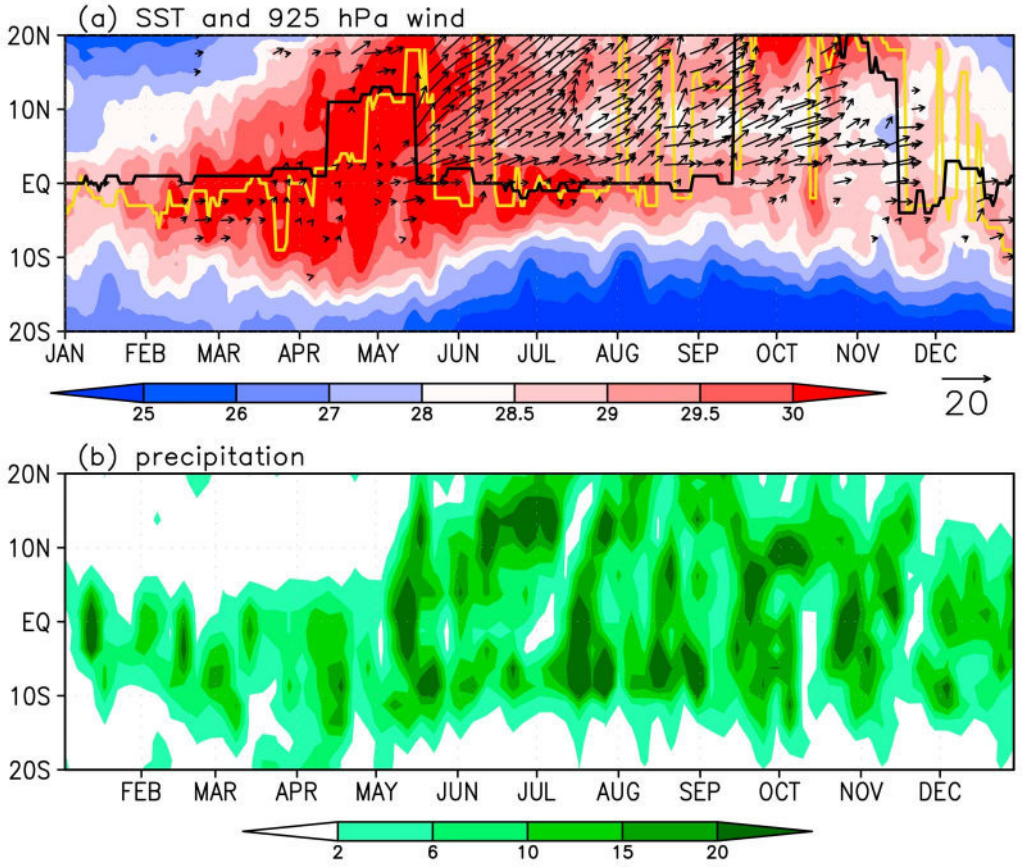

Figure 12. Latitude–time diagrams of longitudinally averaged (a) SST (°C; shading) and wind at 925 hPa, and (b) precipitation (mm d^{-1}) between 85°E and 95°E in 1998. The black (yellow) line represents the position of the meridional SST maximum for the climatology (for 1998).

is mostly ascribed to the longitudinal gradient in meridional wind, with northerly and southerly winds on the north and south sides of the warm SST, caused by the strong MSSTG. In the trade wind region, the annual cycle of SST shows that WSSTA shifts between two local maxima on either sides of the equator or moves slightly north of the equator. Therefore WSSTA has little influence on the local MSSTG and wind direction. However, in the monsoon region, the annual cycle of

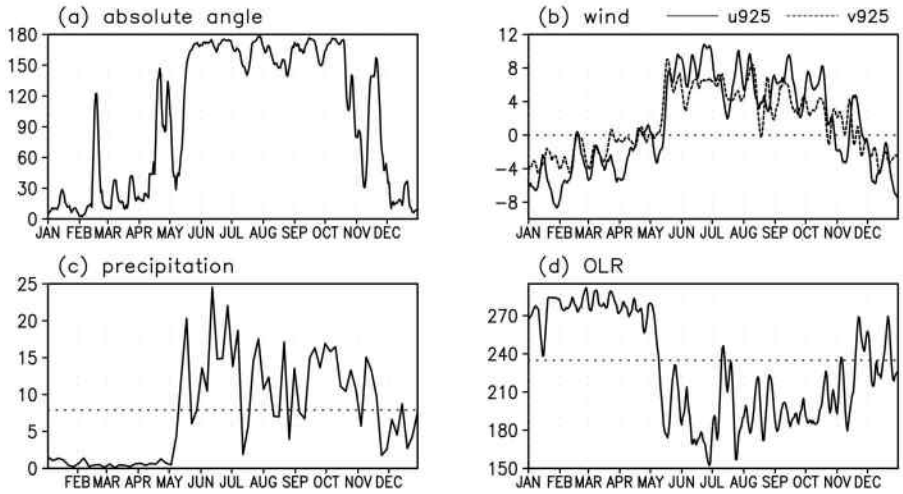

Figure 13. Latitude–time diagrams of the area (5°N–15°N, 85°E–95°E) averaged (a) absolute angle (degrees) of wind vectors at 925 hPa, (b) zonal (ms^{-1}; solid line; u925) and meridional (ms^{-1}; dashed line; v925) components of wind at 925 hPa, (c) precipitation (mm d^{-1}), and (d) OLR (Wm^{-2}) in 1998.

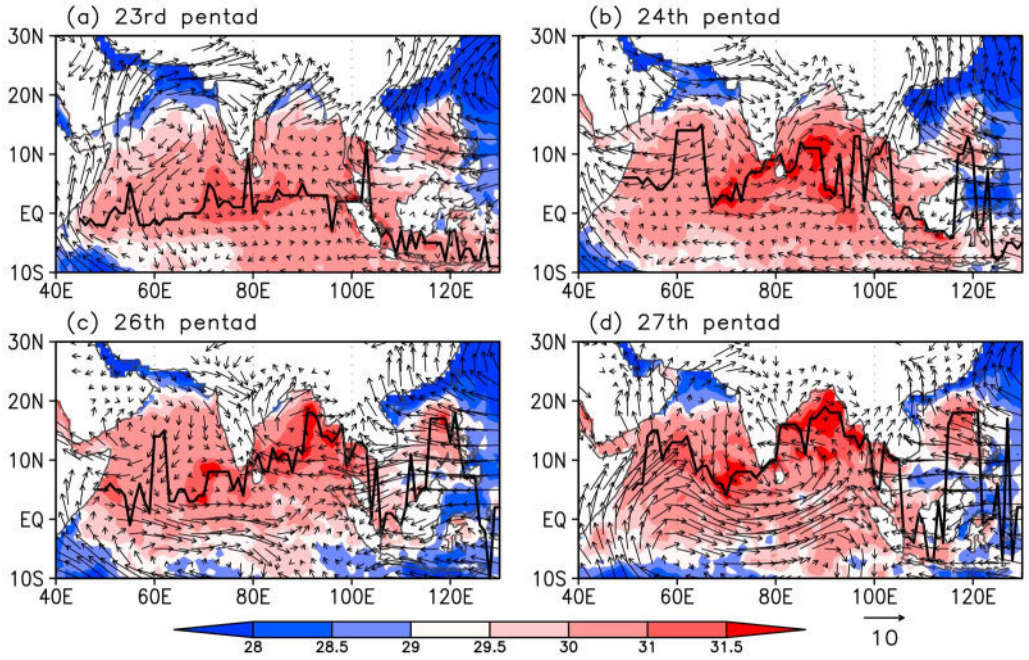

Figure 14. Pentad-mean SST (°C; shading) and wind vectors at 925 hPa in 1998. The thick, solid black line represents the position of the meridional SST maximum.

SST is characterized by large-scale ANJ and ASR of WSSTA, resulting in a marked change in the regional MSSTG and consequent onset of winds. The onset of southwesterlies lags behind the WSSTA jump from the equator to north of 10°N. The timing of this abrupt jump in different regions is coincident with the onset of southwesterlies.

[43] As an example, the climatological onset process of the monsoon in the BOB indicates that the ANJ of WSSTA is caused by an SST increase in the BOB, leading the monsoon onset by about 2 pentads. SST attains a maximum before the monsoon onset, contributing to destabilization of the atmosphere. A strong MSSTG occurs between the BOB and south of the equator, associated with a strong CEF in the equatorial eastern IO. The results of two cases studies indicate that the key climatological features occurred during early and late monsoon onset. The monsoon onset depends mostly on the MSSTG rather than the magnitude of warm SST. An abrupt northward jump of WSSTA, from the equator to north of 10°N, is a good omen for the monsoon onset; the earlier the northward jump, the earlier the monsoon onset.

6.2. Discussion

[44] The annual cycle of SST is generally determined by the annual cycle of solar radiation. Annul mean SST maximum is close to in the equator in the monsoon regions, according to the solar radiation (Figure 1). It has been received less attention compared with the counterpart that in the eastern Pacific and Atlantic, where the maxima are located north of the equator. However, the subseasonal variability of SST maximum is also not consistent with the solar radiation in the monsoon regions, exhibiting ANJ and ASR of WSSTA. The unique feature deserves further study.

[45] *Yano and McBride* [1998] and *Chao* [2000] suggested that before the monsoon onset, there must develop a persistent warm SST far from the equator, based on results obtained using their aqua planet model. In the real complicated climate system, the monsoon onset is also leaded by a persistent SST peak away from the equator. *Sud et al.* [2002] reported that the influence on the monsoon of the annual cycle of solar heating is stronger than that of the annual cycle of SST. The present results also indicate that monsoonal circulation remains strong when the WSSTA retreat southward to the equator. Therefore the land–sea thermal contrast, especially in the Asian monsoon region, is the primary driver of monsoonal circulation. However, SST has a strong influence on subseasonal variability in the monsoon. Even in summer, when the land–sea thermal contrast is the strongest and monsoonal circulation has been firmly established, subseasonal variability in SST plays an important role in the activity and breaking of the monsoon in the BOB [*Vecchi and Harrison*, 2002, *Shankar et al.*, 2007]. Because of the lagged response of the atmosphere to SST, the cooling of SST in the northern BOB precedes the breaking of the monsoon by about 1 week [*Vecchi and Harrison*, 2002]. The present results also indicate that warm SST over the BOB and the location of WSSTA far from the equator (>10°N) lead the monsoon onset, being a good omen for its imminent arrival.

[46] *Mao and Wu* [2007] reported that the interannual variability of the monsoon onset in the BOB is affected by the ENSO. And these occur through changes in the Walker circulation and local Hadley circulation, leading to middle and upper troposphere temperature anomalies over the Asian sector. The case study for 1998 is during a strong El Niño event. The ANJ of WSSTA prior to the monsoon onset in 1998 is later than the climatology, contributed to the late monsoon onset. Thus ENSO may affect the monsoon onset through subseasonal variability of SST. This issue should be addressed in future.

[47] In this study, we investigated the relationship between the annual cycle of SST and the monsoon onset, based on the observational data. Follow-up studies will address the following topics: Why does WSSTA show abrupt jumps and retreats rather than smooth movements consistent with the march of solar radiation? How does the atmosphere respond to the warm SST and MSSTG during the monsoon onset process? Can these features be reproduced by a numerical model? What determines interannual variability of coupled ocean atmosphere processes during the monsoon onset?

[48] **Acknowledgments.** We are grateful to three anonymous referees for their helpful suggestions. This work was jointly supported by the 973 Program (2010CB950400), the NSFC Project (40821092, 41030961), and Basic Research and Operation Program of Institute of Plateau Meteorology, CMA (BROP201017).

References

Chao, W. C. (2000), Multiple quasi equilibria of the ITCZ and the origin of monsoon onset, *J. Atmos. Sci.*, *57*, 641–652, doi:10.1175/1520-0469(2000)057<0641:MQEOTI>2.0.CO;2.

Chao, W. C., and B. Chen (2001), The origin of monsoons, *J. Atmos. Sci.*, *58*, 3497–3507, doi:10.1175/1520-0469(2001)058<3497:TOOM>2.0.CO;2.

Fu, X., B. Wang, and L. Tao (2006), Satellite data reveal the 3-D moisture structure of tropical intraseasonal oscillation and its coupling with underlying ocean, *Geophys. Res. Lett.*, *33*, L03705, doi:10.1029/2005GL025074.

Gadgil, S. (2003), The Indian monsoon and its variability, *Annu. Rev. Earth Planet. Sci.*, *31*, 429–467, doi:10.1146/annurev.earth.31.100901.141251.

Gill, A. E. (1980), Some simple solutions for heat-induced tropical circulation, *Q. J. R. Meteorol. Soc.*, *106*, 447–462, doi:10.1002/qj.49710644905.

He, H., J. W. McGinnis, Z. Song, and M. Yanai (1987), Onset of the Asian monsoon in 1979 and the effect of the Tibetan Plateau, *Mon. Weather Rev.*, *115*, 1966–1995, doi:10.1175/1520-0493(1987)115<1966:OOTASM>2.0.CO;2.

Hung, C., and M. Yanai (2004), Factors contributing to the onset of the Australian summer monsoon, *Q. J. R. Meteorol. Soc.*, *130*, 739–758, doi:10.1256/qj.02.191.

Joseph, P. V., J. K. Eischeid, and R. J. Pyle (1994), Interannual variability of the onset of the Indian monsoon and its association with atmospheric features, El Niño, and sea surface temperature anomalies, *J. Clim.*, *7*, 81–105, doi:10.1175/1520-0442(1994)007<0081:IVOTOO>2.0.CO;2.

Kalnay, E., et al. (1996), The NCEP/NCAR 40-year reanalysis project, *Bull. Am. Meteorol. Soc.*, *77*, 437–471, doi:10.1175/1520-0477(1996)077<0437:TNYRP>2.0.CO;2.

Lau, K., and S. Yang (1997), Climatology and interannual variability of the southeast Asian summer monsoon, *Adv. Atmos. Sci.*, *14*, 141–162, doi:10.1007/s00376-997-0016-y.

Lestari, R. K., and T. Iwasaki (2006), A GCM study on the roles of the seasonal marches of the SST and land-sea thermal contrast in the onset of the Asian summer monsoon, *J. Meteorol. Soc. Jpn.*, *84*, 69–83, doi:10.2151/jmsj.84.69.

Li, C. F., and M. Yanai (1996), The onset and interannual variability of the Asian summer monsoon in relation to land-sea thermal contrast, *J. Clim.*, *9*, 358–375, doi:10.1175/1520-0442(1996)009<0358:TOAIVO>2.0.CO;2.

Li, J., and Q. Zeng (2000), Significance of the normalized seasonality of wind field and its rationality for characterizing the monsoon, *Sci. China, Ser. D*, *43*(6), 646–653.

Li, J., and Q. Zeng (2005), A new monsoon index, its interannual variability and relation with monsoon precipitation, *Clim. Environ. Res.*, *10*(3), 351–365.

Li, J., and L. Zhang (2009), Wind onset and withdrawal of Asian monsoon and their simulated performance in AMIP models, *Clim. Dyn.*, *32*(7–8), 935–968, doi:10.1007/s00382-008-0465-8.

Liebmann, B., and C. A. Smith (1996), Description of a complete (interpolated) outgoing longwave radiation dataset, *Bull. Am. Meteorol. Soc.*, *77*, 1275–1277.

Lindzen, R. S., and S. Nigam (1987), On the role of sea surface temperature gradients in forcing low-level winds and convergence in the tropics, *J. Atmos. Sci.*, *44*, 2418–2436, doi:10.1175/1520-0469(1987)044<2418:OTROSS>2.0.CO;2.

Mao, J., and G. Wu (2007), Interannual variability in the onset of the monsoon over the Eastern Bay of Bengal, *Theor. Appl. Climatol.*, *89*, 155–170, doi:10.1007/s00704-006-0265-1.

Mitchell, T. P., and J. M. Wallace (1992), The annual cycle in equatorial convection and sea surface temperature, *J. Clim.*, *5*, 1140–1156, doi:10.1175/1520-0442(1992)005<1140:TACIEC>2.0.CO;2.

Philander, S. G. H., D. Gu, G. Lambert, T. Li, D. Halpern, N.-C. Lau, and R. C. Pacanowski (1996), Why the ITCZ is mostly north of the equator, *J. Clim.*, *9*, 2958–2972, doi:10.1175/1520-0442(1996)009<2958:WTIIMN>2.0.CO;2.

Reynolds, R. W., T. M. Smith, C. Liu, D. B. Chelton, K. S. Casey, and M. G. Schlax (2007), Daily high-resolution blended analyses for sea surface temperature, *J. Clim.*, *20*, 5473–5496, doi:10.1175/2007JCLI1824.1.

Shankar, D., S. Shetye, and P. Joseph (2007), Link between convection and meridional gradient of sea surface temperature in the Bay of Bengal, *J. Earth Syst. Sci.*, *116*, 385–406, doi:10.1007/s12040-007-0038-y.

Sud, Y. C., G. K. Walker, V. M. Mehta, and W. K.-M. Lau (2002), Relative importance of the annual cycles of sea surface temperature and solar irradiance for tropical circulation and precipitation: A climate model simulation study, *Earth Interact.*, *6*, 1–32, doi:10.1175/1087-3562(2002)006<0001:RIOTAC>2.0.CO;2.

Ueda, H. (2005), Air-sea coupled process involved in stepwise seasonal evolution of the Asian summer monsoon, *Geogr. Rev. Jpn.*, *78*, 825–841.

Vecchi, G. A., and D. E. Harrison (2002), Monsoon breaks and subseasonal sea surface temperature variability in the Bay of Bengal, *J. Clim.*, *15*, 1485–1493, doi:10.1175/1520-0442(2002)015<1485:MBASSS>2.0.CO;2.

Wang, B. (2006), *The Asian Monsoon*, 1st ed., 328 pp., Springer, Berlin.

Wang, B., and L. Ho (2002), Rainy season of the Asian-Pacific summer monsoon, *J. Clim.*, *15*, 386–398, doi:10.1175/1520-0442(2002)015<0386:RSOTAP>2.0.CO;2.

Wang, B., Q. Ding, and P. V. Joseph (2009), Objective definition of the Indian monsoon onset, *J. Clim.*, *22*, 3303–3316, doi:10.1175/2008JCLI2675.1.

Webster, P. J., V. O. Magaña, T. N. Palmer, J. Shukla, R. A. Tomas, M. Yanai, and T. Yasunari (1998), Monsoons: Processes, predictability, and the prospects for prediction, *J. Geophys. Res.*, *103*, 14,451–14,510, doi:10.1029/97JC02719.

Wu, G., and Y. Zhang (1998), Tibetan Plateau forcing and the timing of the monsoon onset over south Asia and the South China Sea, *Mon. Weather Rev.*, *126*, 913–927, doi:10.1175/1520-0493(1998)126<0913:TPFATT>2.0.CO;2.

Wu, R. (2010), Subseasonal variability during the South China Sea monsoon onset, *Clim. Dyn.*, *34*, 629–642, doi:10.1007/s00382-009-0679-4.

Wu, R., and B. Wang (2000), Interannual variability of monsoon onset over the western North Pacific and the underlying processes, *J. Clim.*, *13*, 2483–2501, doi:10.1175/1520-0442(2000)013<2483:IVOSMO>2.0.CO;2.

Wu, R., and B. Wang (2001), Multi-stage onset of the monsoon over the western North Pacific, *Clim. Dyn.*, *17*, 277–289, doi:10.1007/s003820000118.

Xie, P., and P. A. Arkin (1997), Global precipitation: A 17-year monthly analysis based on gauge observations, satellite estimates, and numerical model outputs, *Bull. Am. Meteorol. Soc.*, *78*, 2539–2558, doi:10.1175/1520-0477(1997)078<2539:GPAYMA>2.0.CO;2.

Xie, S.-P. (1994), On the genesis of the equatorial annual cycle, *J. Clim.*, *7*, 2008–2013, doi:10.1175/1520-0442(1994)007<2008:OTGOTE>2.0.CO;2.

Xie, S.-P., and S. G. H. Philander (1994), A coupled ocean-atmosphere model of relevance to the ITCZ in the eastern Pacific, *Tellus, Ser. A*, *46*, 340–350.

Yanai, M. H., C. F. Li, and Z. S. Song (1992), Seasonal heating of the Tibetan Plateau and its effects on the evolution of the Asian summer monsoon, *J. Meteorol. Soc. Jpn.*, *70*, 319–351.

Yano, J.-I., and J. L. McBride (1998), An aquaplanet monsoon, *J. Atmos. Sci.*, *55*, 1373–1399, doi:10.1175/1520-0469(1998)055<1373:AAM>2.0.CO;2.

Zeng, Q., and J. Li (2002), On the interaction between Northern and Southern Hemispheric atmospheres and the essence of tropical monsoon, *Chinese J. Atmos. Sci.*, *26*, 207–226.

Zhang, L., and J. Li (2008), Seasonal rotation features of wind vectors and application to evaluate monsoon simulations in AMIP models, *Clim. Dyn.*, *31*(4), 417–432, doi:10.1007/s00382-007-0327-9.

Zhang, L., and J. Li (2010), Twice wind onsets of monsoon over the western north Pacific and their simulations in AMIP models, *Int. J. Climatol.*, *30*, 582–600, doi:10.1002/joc.1908.

Zhang, Y., T. Li, B. Wang, and G. Wu (2002), Onset of the monsoon over the Indochina Peninsula: Climatology and interannual variations, *J. Clim.*, *15*, 3206–3221, doi:10.1175/1520-0442(2002)015<3206:OOTSMO>2.0.CO;2.

X. Jiang and J. Li, State Key Laboratory of Numerical Modeling for Atmospheric Sciences and Geophysical Fluid Dynamics, Institute of Atmospheric Physics, Chinese Academy of Sciences, Beijing 100029, China. (ljp@lasg.iap.ac.cn; dqjxw@yahoo.com.cn)